Electrochimica Acta 261 (2018) 307–313

Contents lists available at ScienceDirect

Electrochimica Acta

journal homepage: www.elsevier.com/locate/electacta

Observation of ionic hydrogen bonding between anions and triarylamine-based aromatic polyimides with secondary amine

Hung-Ju Yen [a, 1, 2], Jhe-Huang Lin [a, 1], Yuhlong Oliver Su [b], Guey-Sheng Liou [a, *]

[a] Institute of Polymer Science and Engineering, National Taiwan University, 1 Roosevelt Road, 4th Sec., Taipei, 10617, Taiwan
[b] Department of Applied Chemistry, National Chi Nan University, Puli, Nantou, 54561, Taiwan

ARTICLE INFO

Article history:
Received 13 September 2017
Received in revised form
23 December 2017
Accepted 25 December 2017
Available online 29 December 2017

Keywords:
Anion detection
Polyimide
Secondary amine
Hydrogen bond
Triphenylamine

ABSTRACT

Four triarylamine-based high-performance polyimides with secondary amine were readily synthesized, their ionic hydrogen-bonding interaction with pyridines and anions are successfully demonstrated (20 times higher than the literature in sensitivity) by the means of electrochemistry and spectroelectrochemistry. The prepared polymer thin films having the advantage for real-time qualitative detection are great candidates as chemosensors to both pyridines and anions.

1. Introduction

Nowadays, highly sensitive and reliable anion detectors are urgent in demand because of the degenerative environment and increasing biological and chemical threats. For example, fluoride is a well-known essential element for dental care. Nevertheless, an excess amount of fluoride will cause severe problem to tooth and bone, even be harmful for body health, such as urolithiasis (kidney stone disease), skeleton fluorosis, and at worst scenario, lethal [1]. Therefore, increased safety methods are needed for operational support in responding to hazardous emergency issues. The ability to timely detect, identify and monitor fluoride anion or hazardous material is imperative for the effective usage of both civilian defense and military resources. For this reason, lots of chemosensors have been synthesized and reported [2–4], taking the rapidly formed hydrogen-bonding between chemosensors and target anions into consideration [5,6]. Fluorescent and colorimetric detections are the most widely applied approaches for anion detection. However, the *ideal detector* has not been a reality for commercialization due to the limited methods and low sensitivity [7,8]. The other major challenge is the demand for increasing detection reliability and reducing the frequency of falseness.

Since 1996, Linschitz [9] and Smith [10–14] have done significant efforts to elucidate the redox-dependent formation through electrochemically controlled hydrogen bonding between the reductive compounds and hydrogen donors, such as water, amides, alcohol, acids and ureas. Recently, Su's group [15] systematically reported a series of phenylenediamines exhibiting redox potential inversion resulted from the ionic hydrogen bonds with pyridines or alcohols. The potential shift (the new redox couple $E_2^{ox\prime}$ is obviously lower than E_1^{ox}) could be classified as *potential inversion* [16] with a single two-electron wave, which is rare and mostly accompanied with significantly structural change [17–19], large solvation [20] or redox potential shifts by ionic H-bonding [9,21]. Nevertheless, these compounds are very rare and their low potential shifts usually performed negligible signals (<50 mV at 1 equiv. of anion) [22].

In this work, we are exploring new enabled measuring approaches for anion sensing applications by applying a series of aromatic imides and polyimides (PIs) with secondary amine structures as molecular recognition elements via electrochemical and spectroelectrochemical transduction technologies. The successful introduction of packing-disruptive triarylamine moieties into the polymer main chain is essential for fabricating patternable thin-film sensors by jet-printing and spin-coating methods. The

* Corresponding author.
E-mail address: gsliou@ntu.edu.tw (G.-S. Liou).
[1] H.-J. Yen and J.-H. Lin contributed equally.
[2] Present address: Institute of Chemistry, Academia Sinica, Taipei, Taiwan.

https://doi.org/10.1016/j.electacta.2017.12.157
0013-4686/

schematic illustration of stabilizing the cation radical through hydrogen bonding between secondary amines and pyridines/anions is depicted in Fig. 1, as well as the summary of the pK_a values of pyridines and their hydrogen-bond binding strength. The ultimate goal of our research efforts is to develop a field of deployable detection capability for anions and hazardous materials that is fast, accurate and sensitive.

2. Results and discussion

2.1. Polymer synthesis

Aromatic PIs containing secondary amines were synthesized by the conventional one-step imidization of diamines with secondary amine [23] and two commercial dianhydrides in *m*-cresol at 185 °C with catalytic amount of isoquinoline (Scheme 1). The polymerization reaction proceeded smoothly and the obtained PIs with inherent viscosities of 0.46–0.61 dL/g can be solution-cast into tough, flexible, and free-standing films (see inset figure of Scheme 1), revealing the successful preparation of high molecular weight PIs (Table S1).

The IR spectra of PIs **H**–**6F** and **H-DS** shown in Fig. S1 exhibited characteristic imide absorption bands at around 1780 and (C=O), 1721 (C=O), 1380 (C–N), 740 (imide ring deformation), and secondary amine at 3390 cm^{-1}. ^{1}H NMR spectra of the prepared PIs are illustrated in Fig. 2. No resonance peaks appeared from 9 to 12 ppm in the ^{1}H NMR spectra further supports the complete imidization of all the PIs. The results identified by IR and NMR spectroscopic techniques are in perfect agreement with the proposed structures.

In order to obtain simplified structural information of the PIs, the model compounds with secondary amine groups were also synthesized by the condensation of their corresponding diamine monomers and two equivalent amounts of phthailic anhydride (Scheme 2). Their FT-IR and ^{1}H NMR spectra are shown in Figs. S2 and S3, respectively. The obtained model compounds were used for electrochemical and spectroelectrochemical measurement.

2.2. Basic characterization of polyimides

The solubility properties of PIs were tested quantitatively and summarized in Table S2. These polymers are soluble in various solvents. The PIs prepared from dianhydride 6FDA exhibited higher solubility than those from DSDA owing to the bulky hexafluoroisopropylidene linkage in the polymers that is beneficial for practical fabrication of high performance optoelectronic devices.

The thermal behaviors of the synthesized PIs were investigated by TGA and TMA, and the results are tabulated in Table S3. The PIs were thermally stable up to 425 °C (depicted in Fig. S4) and the carbonized residue in nitrogen was more than 55% at 800 °C, estimating LOI values up to 42. The softening temperature (T_s) could be measured by TMA thermograms (as shown in Fig. S5). These PIs revealed remarkably high T_s as a result of the present rigid aromatic units. Moreover, DSDA-based PIs exhibited higher T_s due to the higher intermolecular force and strong dipole interactions contributed from the sulfone group, thus restricting the rotation and movement of the polymer chains. The results suggested that the high aromatic content is beneficial for thermal stability and behavior of the prepared PIs.

2.3. Electrochemical properties and in-situ UV–vis absorption

The electrochemical sensing technology relies on the ability of anion or hazardous materials to be bound with anionic products by H-bonding, which can be monitored and measured through a small electric current or potential shift at the surface of an electrode. This change is normally monitored through an electrode. Specificity to a target is provided by optimization of the electrochemistry. Furthermore, quantification of the anion or hazardous materials can be determined by the electrical current produced. The electrochemistry was studied by cyclic voltammetry (CV). Model compounds (10 μmol) were dissolved in dichloromethane with 0.1 M of tetrabutylammonium perchlorate (TBAP) as an electrolyte and glassy carbon disk is used as working electrode. Besides, the polymers were conducted by casting film (0.55 cm^2 in area) on an ITO-coated glass as working electrode.

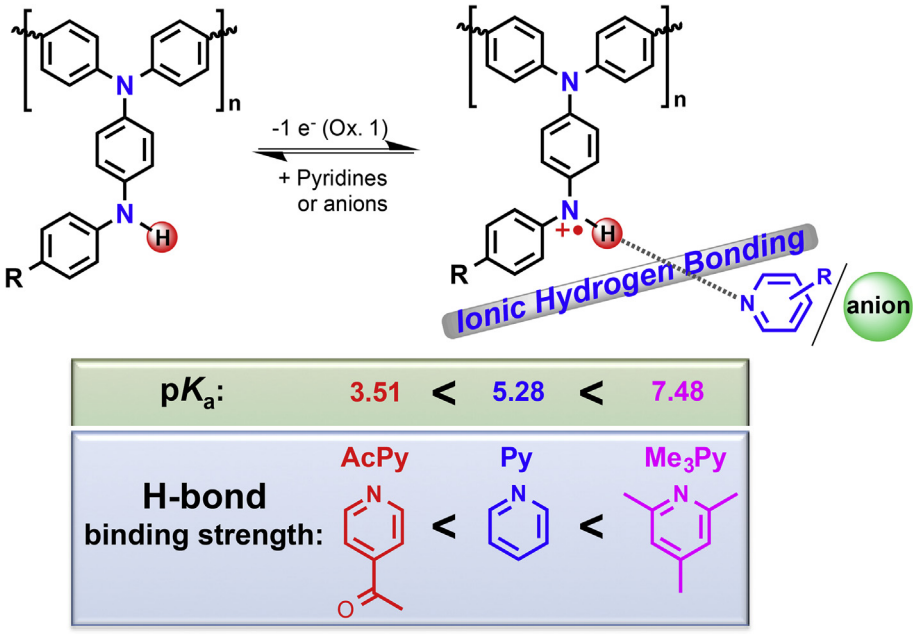

Fig. 1. Schematic illustration of stabilizing the cation radical through hydrogen bonding between secondary amines and pyridines/anions. Summary of the pK_a values of pyridines as well as their hydrogen-bond binding strength. (AcPy: 4-acetylpyridine; Py: pyridine; Me_3Py: 2,4,6-trimethylpyridine).

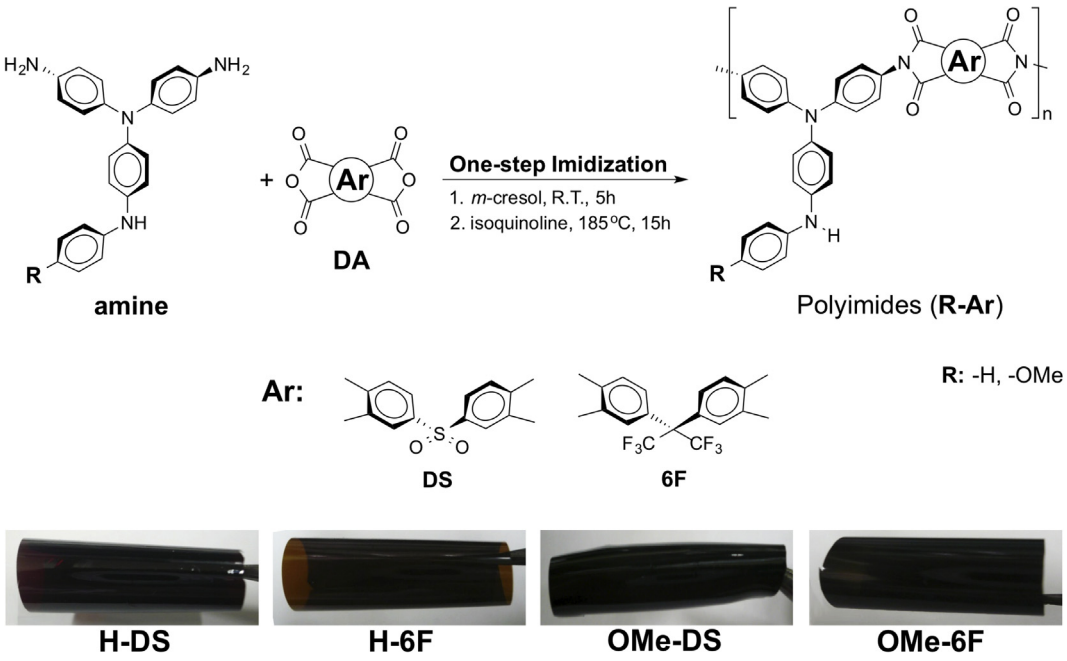

Scheme 1. Synthesis, structure, and appearance of PI films.

2.3.1. Characterization of model compounds

In Fig. 3, compounds **M-H** and **M-OMe** both exhibited two reversible oxidation redox couples before adding pyridines, which is called "***normal potential***" resulted from the strong electronic coupling (the electron is delocalized over the two redox centers) between two nitrogen atoms. Therefore, the nitrogen of the secondary amine is electron richer than the N atom on the other side, and will be oxidized easier than the one from the triphenylamine core (Fig. S6a). Moreover, compound **M-OMe** ($E_1^{ox} = 0.63$ V; $E_2^{ox} = 1.09$ V) exhibited lower oxidation potentials than that of compound **M-H** ($E_1^{ox} = 0.71$ V; $E_2^{ox} = 1.17$ V) due to the inductive effect of the substituent [24] by changing the *para*-substitution from hydrogen atom to an electron-donating methoxy group, indicating the more basicity of **M-OMe** than that of **M-H**.

After AcPy ($pK_a = 3.51$, Fig. 3a) was added to the solution of **M-H**, a new oxidation wave ($E_2^{ox\prime} = 1.0$ V) grows and the current at $E_2^{ox} = 1.18$ V gradually decreased. As AcPy reached 1 equiv. (10.0 μmole) to **M-H**, oxidation couple of E_2^{ox} disappeared completely and the appearance of $E_2^{ox\prime}$ is considered as the new second oxidation, which is attributed to the interaction between **M-H** and AcPy. Besides, Py ($pK_a = 5.28$; Fig. 3c and d) only further lowered the $E_2^{ox\prime}$, seeming to merge with E_1^{ox}, but didn't shift the E_1^{ox} even with equivalent to model compounds **M**.

Moreover, when Me_3Py ($pK_a = 7.48$, Fig. 3e) was applied to **M-H**, the CV exhibited different redox patterns to other pyridines. The new redox wave produced at a much lower potential even than E_1^{ox}. The final CV curve (blue solid line of Fig. 3e) with 1 equiv. (10.0 μmole) of Me_3Py showed only one redox couple at $E_2^{ox\prime} = 0.66$ V, which is obviously lower than E_1^{ox}. Importantly, the final peak current is about *2 times higher than the first one*, suggesting that the H-bonding is significantly stabilizing the oxidized product. We further performed the absorbance measurement by addition of donor acceptor (pyridines or anion) without applying the potential to confirm the hydrogen bonding interaction. As the results shown in Fig. S7, Me_3Py serves as an acceptor to the secondary amine, therefore a small IVCT band was formed according to the electron transfer from active neutral nitrogen atom to the pyridine-bounded nitrogen.

While, the fairly basic H-bonding molecules (e.g. fluoride, acetate, carbonate anions etc) with the similar potential shifts have never been explored. Thus, the interaction of fluoride and acetate anions was further performed and demonstrated the high sensitivity of these synthesized materials. As summarized in Fig. 4, acetate and fluoride anions are slowly added into the solution of model compounds. The final CV curves (blue solid lines in Fig. 4) all showed only one new redox couple $E_2^{ox\prime}$ at around 0.55–0.64 V, which are apparently lower than E_1^{ox} owing to the H-bonding interaction. The larger potential shifts in fluoride anion than in acetate anion could be attributed to the smaller size and stronger electrostatic attraction of fluoride anion, resulting in stronger binding strength of the ionic hydrogen bonding.

Moreover, *in-situ* UV–vis spectra of **M-OMe**$^{+\bullet}$ is performed to confirm the presence of H-bonding during adding fluoride anion. This technology is based upon specific chemical reactions that occur when anions interact with the sensors. The amount of light absorbed in a sample can be used to determine the amount of anion in the sample. It is possible to derive a graph that shows the absorption characteristics of a sample by using this information. Spectra can be used for identifying an unknown anion, and in some cases can unambiguously determine the identity of the species. Also, 0.60 V was set to achieve the cation radical for confirming the ionic hydrogen bonding with pyridines or anions. Absorption spectra change in Fig. 5a indicated that the **M-OMe**$^{+\bullet}$ exhibited a broad IV-CT band in the NIR region due to the excitation between states where the positive charge was centered at different nitrogen atoms [25].

After fluoride anion was added to **M-OMe**$^{+\bullet}$, the absorption peak at 680 nm gradually increased in intensity, and a broad band centered at 405 and 940 nm decreased. The disappearance of NIR absorption as well as the new band centered at 680 nm was resulted from the formation of dication in the *N,N,N′*-triphenylbenzene-*para*-diamine segments. Without adding fluoride anion, **M-OMe** exhibited strong absorption at around 330 nm, characteristic for triarylamine unit at the neutral form (0 V). Upon oxidation (increasing applied voltage from 0 to 0.6 V), the intensity of the absorption peak at 330 nm gradually decreased while a new shoulder at 405 nm and a broad band having its maximum

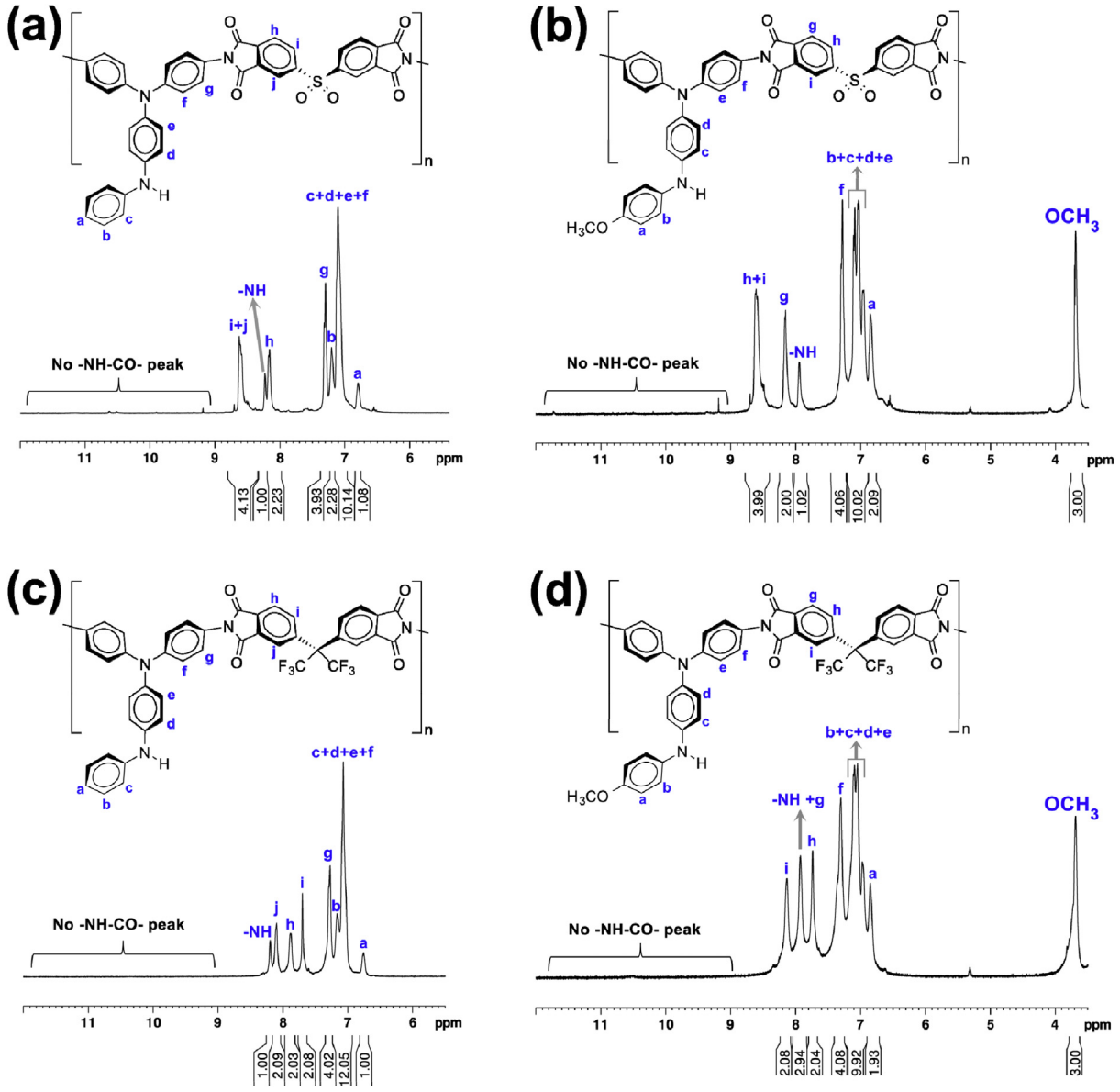

Fig. 2. ^{1}H NMR spectra of PIs (a) **H-DS**, (b) **OMe-DS** (c) **H**–**6F** and (d) **OMe**–**6F** in DMSO-d_6.

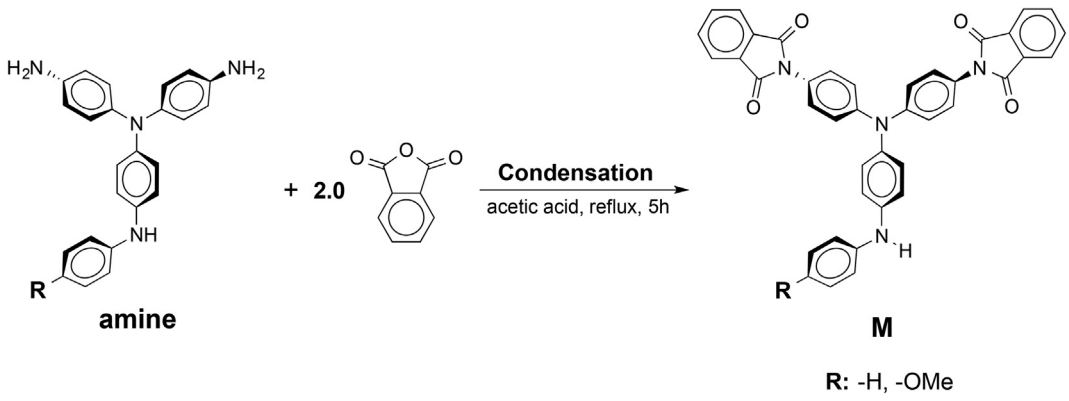

Scheme 2. Synthetic route to model compounds.

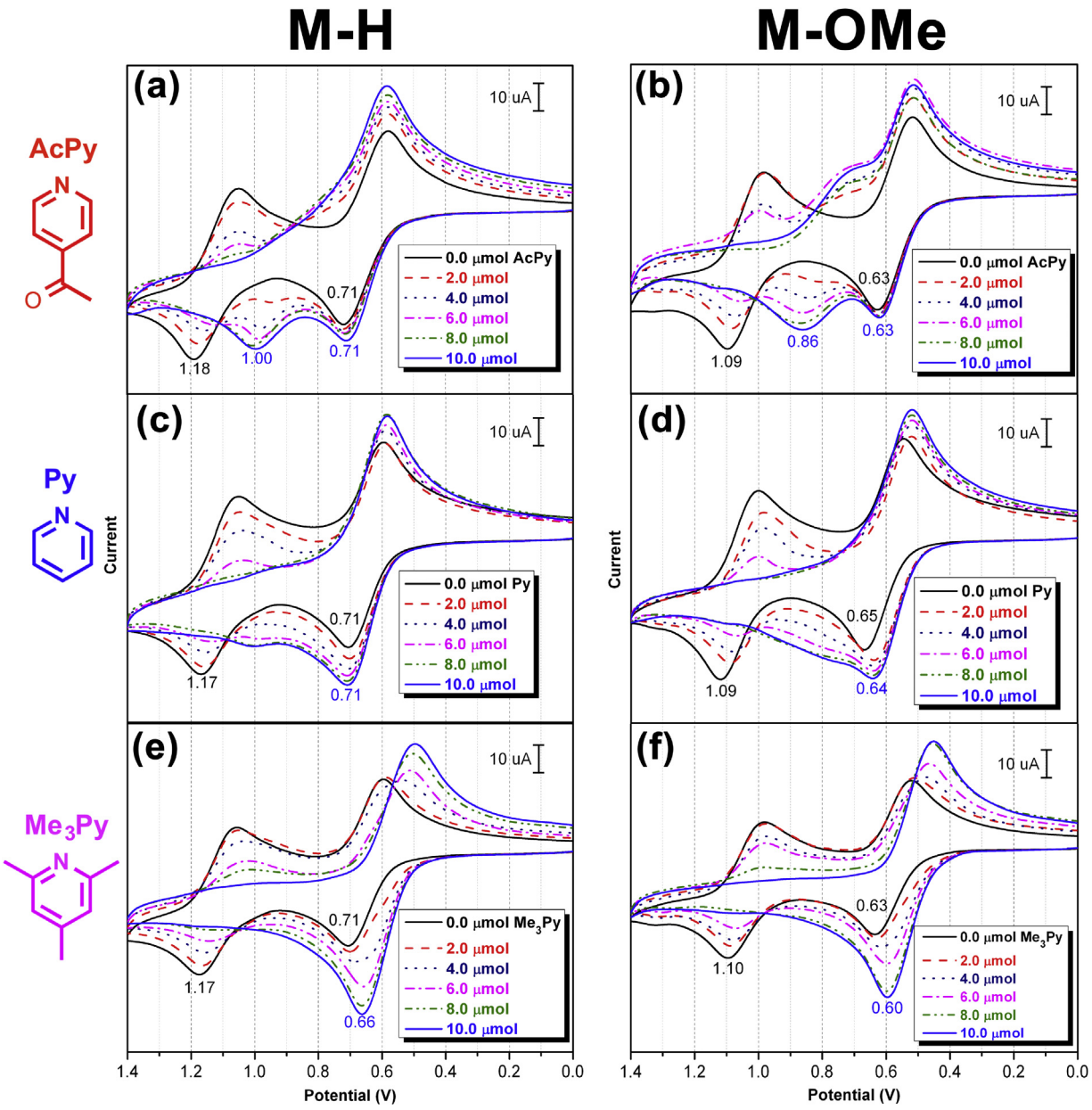

Fig. 3. Cyclic voltammograms of 10 μmol **M-H** (a,c,e) and **M-OMe** (b,d,f) in 0.1 M TBAP/dichloromethane with various amount of (a and b) AcPy [pK_a = 3.51], (c and d) Py [pK_a = 5.28] and (e and f) Me_3Py [pK_a = 7.48]. Scan rate: 100 mV/s. Working electrode: glassy carbon disk (area = 0.07 cm^2).

absorption wavelength at 940 nm in the NIR region gradually increased in intensity. As the anodic potential increasing to 1.20 V, the absorption bands of the cation radical decreased gradually with a new broad band centered at around 680 nm. The disappearance of NIR absorption band can be attributed to the further oxidation of monocation radical species to the formation of dication (Fig. S6b). Since the applied potential of spectroelectrochemistry was set to be 0.60 V, the set potential is considered to be high enough to oxidize both of the electron-active centers "after the H-bonding interaction". Therefore, we attribute the new band centered at 680 nm was caused by the formation of dication, especially at a relatively low applied potential of 0.60 V. Interestingly, as summarized in Fig. 5b, after added only 0.2 equivalent of fluoride anion to **M-OMe**, the disappearance of IV-CT band strongly confirms the H-bonding interaction between **M-OMe**$^{+\bullet}$ and fluoride anion. Further adding the fluoride anion leads to the stronger H-bonding interaction and fully oxidation of **M-OMe** at 0.60 V, which is proven by the gradually increased absorption peak at 680 nm.

2.3.2. Characterization of polyimides

The shift of E_2^{ox} for model compounds indicates the different interaction force between the secondary amine and pyridines/anions, which was affected by the strength of H-bonding. The corresponding PI has the similar electrochemical result as well (Fig. 6). The CV curve of PI **OMe**–**6F** showed two reversible oxidation waves at E_1^{ox} = 0.73 V and E_2^{ox} = 1.08 V, respectively (black solid line). After Me_3Py was added to the solution, the final $E_2^{ox\prime}$ is also lower than E_1^{ox} and the peak current is around 2 times higher than E_1^{ox}. This H-bonding interaction is relatively similar to the structure-related compounds. Moreover, the CV diagrams and absorption spectra change of **OMe**–**6F**$^{+\bullet}$ after adding fluoride anion were also presented in Fig. 6b and c to demonstrate the strength of H-bonding

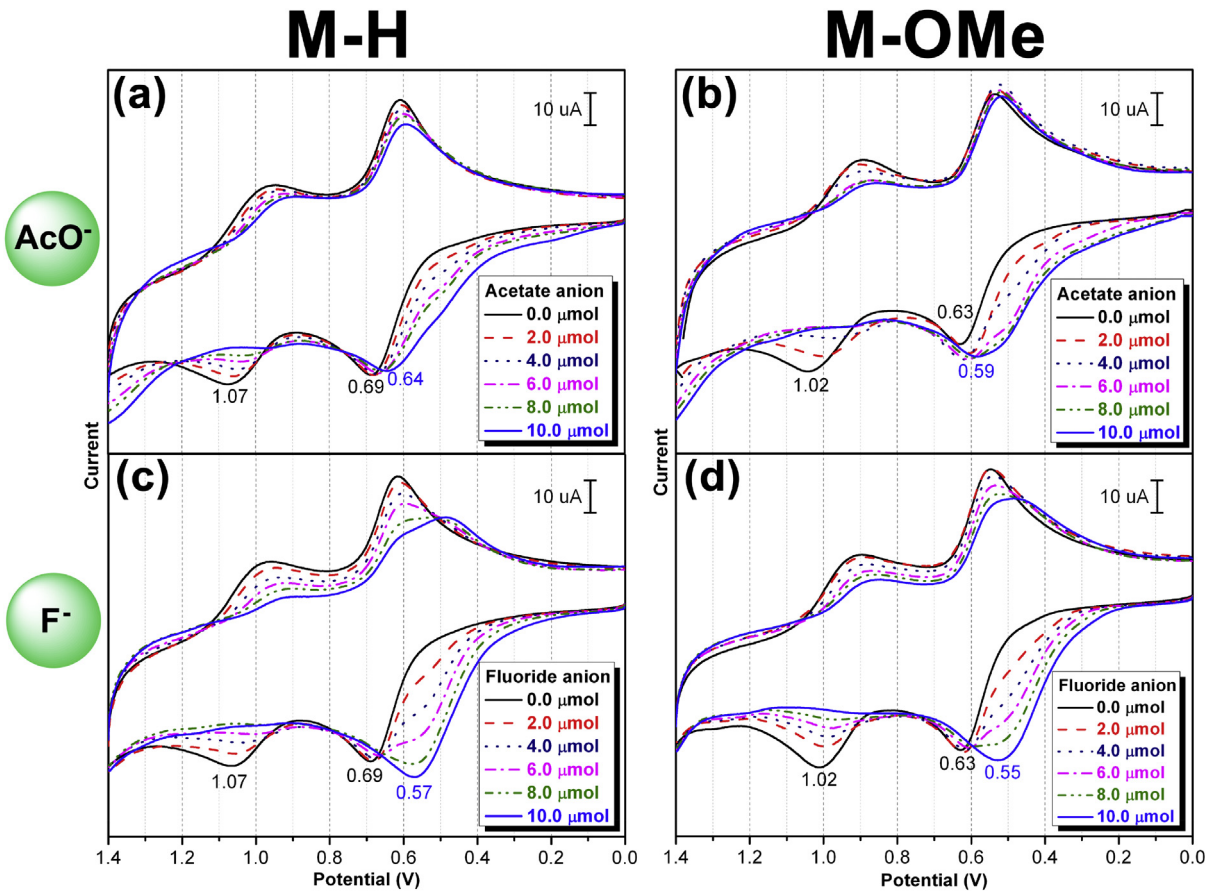

Fig. 4. Cyclic voltammograms of 10 μmol **M-H** (a,c) and **M-OMe** (b,d) in 0.1 M TBAP/dichloromethane with various amount of (a and b) acetate anion, (c and d) fluoride anion. Scan rate: 100 mV/s. Working electrode: glassy carbon disk (area = 0.07 cm^2).

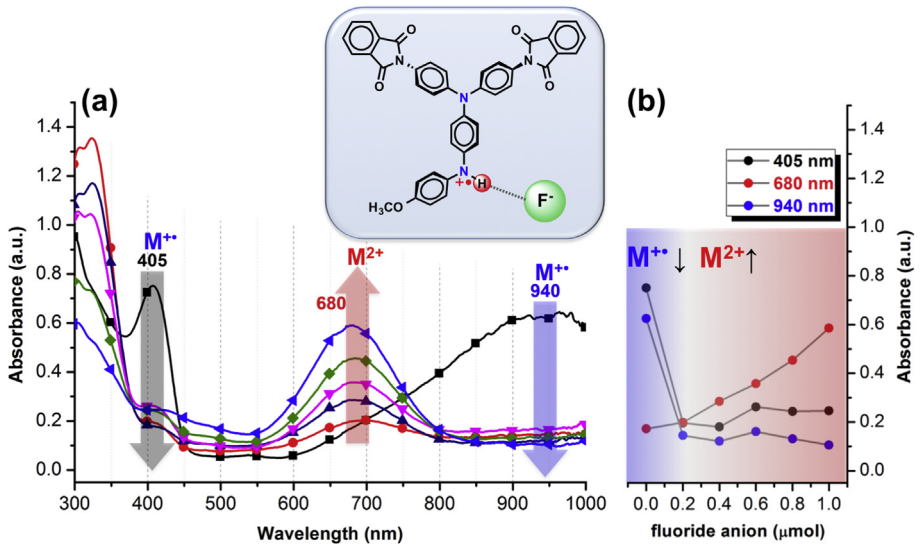

Fig. 5. (a) Absorption spectra change of 1.0 μmol **M-OMe** in 0.1 M TBAP/dichloromethane with various amount of fluoride anion (added from 0 with 0.2 μmol interval) at 0.60 (V vs. Ag/AgCl). (b) Absorbance change monitored at the given wavelength with various amount of fluoride anion.

between **OMe**–**6F**$^{+\bullet}$ and fluoride anion accordingly. The disappearance of IV-CT band centered at 890 nm illustrates the H-bonding formation, and the new peak generated at around 660 nm implies the H-bonding interaction and fully oxidation of **OMe**–**6F** at 0.70 V, which displays a perfect consistency with Fig. 5a.

Although the model compounds have demonstrated remarkable performance both in qualitative and quantitative interactions on pyridines and anions, even performed a much higher detection ability (up to 500 mV) compared to the reported literature (20 mV) at 1equiv. of anion [22]. However, the detection by compounds in solution-state would not be an ideal and practical approach; instead, the polymeric detector can successfully address this issue. Solid-state polymer thin films prepared in this work contribute tremendous advantages for the real-time qualitative detection;

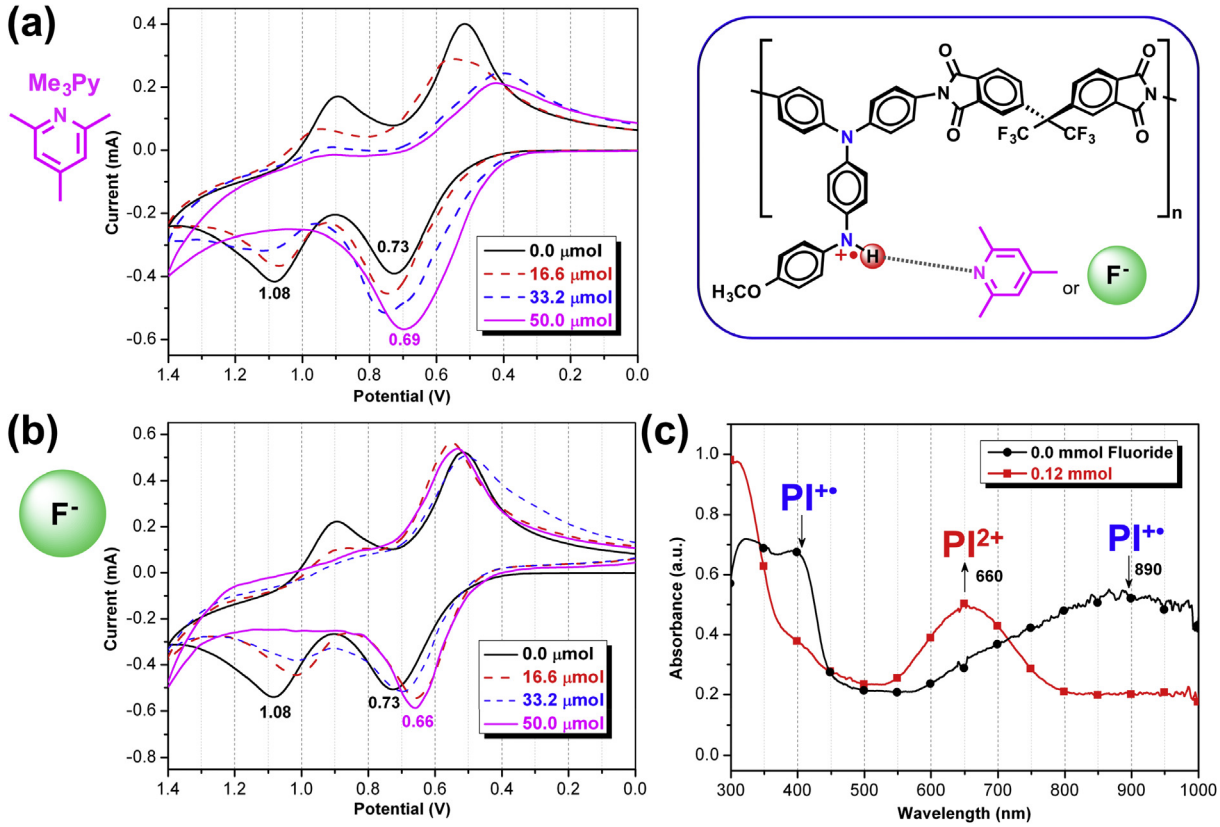

Fig. 6. The shift of second potential for **OMe–6F** with various amount of (a) Me_3Py [$pK_a = 7.48$] and (b) fluoride anion in 0.1 M TBAP/CH_3CN. Scan rate: 100 mV/s. (c) The absorption spectra of **OMe–6F**$^{+\bullet}$ in presence of fluoride anion in 0.1 M TBAP/CH_3CN at 0.70 (V vs. Ag/AgCl).

thus, these polymeric materials, adopting this interesting concept and facile approach, are promising candidates as practical chemosensors for both pyridines and anions.

3. Conclusions

Four triarylamine-based high-performance PIs were synthesized and their sensing ability to pyridines and anions was investigated and reported. The electrochemical and spectroelectrochemical results demonstrated that the secondary amine on triarylamine-based PIs effectively interacts with proton acceptor to form ionic H-bonding. This work also contributes the capability in addressing anion or hazardous materials sensing to ultimately enable better designing and understanding for molecular structure evolution and discovery.

Acknowledgements

The authors are grateful acknowledge to the Ministry of Science and Technology of Taiwan for the financial support.

Appendix A. Supplementary data

Supplementary data related to this article can be found at https://doi.org/10.1016/j.electacta.2017.12.157.

References

[1] G.B. Reddy, A.L. Khandare, P.Y. Reddy, G.S. Rao, N. Balakrishna, I. Srivalli, Toxicol. Sci. 72 (2003) 363–368.
[2] Y. Zhou, J.F. Zhang, J. Yoon, Chem. Rev. 114 (2014) 5511–5571.
[3] P.A. Gale, C. Caltagirone, Chem. Soc. Rev. 44 (2015) 4212–4227.
[4] R. Sakai, T. Satoh, T. Kakuchi, Polym. Rev. 57 (2017) 159–174.
[5] C. Wang, G. Li, Q. Zhang, Tetrahedron Lett. 54 (2013) 2633–2636.
[6] I.S. Turan, E.U. Akkaya, Org. Lett. 16 (2014) 1680–1683.
[7] Y. Shiraishi, S. Sumiya, T. Hirai, Chem. Commun. 47 (2011) 4953–4955.
[8] B. Hu, P. Lu, Y. Wang, Sens. Actuator B Chem. 195 (2014) 320–323.
[9] N. Gupta, H. Linschitz, J. Am. Chem. Soc. 119 (1997) 6384–6391.
[10] Y. Ge, L. Miller, T. Ouimet, D.K. Smith, J. Org. Chem. 65 (2000) 8831–8838.
[11] Y. Ge, R.R. Lilienthal, D.K. Smith, J. Am. Chem. Soc. 118 (1996) 3976–3977.
[12] Y. Ge, D.K. Smith, Anal. Chem. 72 (2000) 1860–1865.
[13] J. Bu, N.D. Lilienthal, J.E. Woods, C.E. Nohrden, K.T. Hoang, D. Truong, D.K. Smith, J. Am. Chem. Soc. 127 (2005) 6423–6429.
[14] C. Chan-Leonor, S.L. Martin, D.K. Smith, J. Org. Chem. 70 (2005) 10817–10822.
[15] Y.-C. Chung, Y.-J. Tu, S.-H. Lu, W.-C. Hsu, K.Y. Chiu, Y.O. Su, Org. Lett. 13 (2011) 2826–2829.
[16] A. Nafady, T.T. Chin, W.E. Geiger, Organometallics 25 (2006) 1654–1663.
[17] N.A. Macías-Ruvalcaba, D.H. Evans, J. Phys. Chem. B 110 (2006) 5155–5160.
[18] D.H. Evans, K. Hu, J. Chem. Soc. Faraday Trans. 92 (1996) 3983–3990.
[19] R.L. Lord, F.A. Schultz, M.-H. Baik, Inorg. Chem. 49 (2010) 4611–4619.
[20] P. Hapiot, L.D. Kispert, V.V. Konovalov, J.-M. Savéant, J. Am. Chem. Soc. 123 (2001) 6669–6677.
[21] E. Martinez-Gonzalez, F.J. Gonzalez, J.R. Ascenso, P.M. Marcos, C. Frontana, J. Org. Chem. 81 (2016) 6329–6335.
[22] N.H. Evans, P.D. Beer, Org. Biomol. Chem. 9 (2011) 92–100.
[23] H.-J. Yen, J.-H. Lin, Y.O. Su, G.-S. Liou, J. Mater. Chem. C 4 (2016) 10381–10385.
[24] H.-J. Yen, G.-S. Liou, Chem. Mater. 21 (2009) 4062–4070.
[25] Y.-W. Chuang, H.-J. Yen, G.-S. Liou, Chem. Commun. 49 (2013) 9812–9814.